

THE EFFECT OF CaO ON THE RECOVERY OF Fe AND Ni IN A VACUUM CARBOTHERMAL REDUCTION OF GARNIERITE

Q. Wang^{b,c,d}, T. Qu^{a,b,c,d*}, X.-P. Gu^{a,b,c,d}, L. Shi^{b,c,d}, B. Yang^{a,b,c,d}, Y.-N. Dai^{b,c,d}

^a State Key Laboratory of Complex Non-ferrous Metal Resources Clear Utilization, Kunming University of Science and Technology, Kunming, China

^b National Engineering Laboratory for Vacuum Metallurgy, Kunming University of Science and Technology, Kunming, China

^c Key Laboratory of Vacuum Metallurgy for Nonferrous Metal of Yunnan Province, Kunming University of Science and Technology, Kunming, China

^{d*} Faculty of Metallurgical and Energy Engineering, Kunming University of Science and Technology, Kunming, China

(Received 13 February 2019; accepted 13 June 2019)

Abstract

The effects of adding CaO during a vacuum carbothermal reduction on Fe and Ni recovery yields were examined. In addition, magnetic separation was investigated. Experiments were conducted under pressures ranging from 10 to 50 Pa with different proportions of CaO at different temperatures. The results indicated that at 1723 K, the mass ratio of ore/C was 100:65.5; when the amount of CaO was 22.64% (the mole ratio of CaO/Si was 1:1), the recovery of Fe and Ni reached 84.33% and 97.00% in the vacuum carbothermal reduction-magnetic separation process, and the enrichment ratios of Fe and Ni were maximized, reaching 6.32 and 6.72, respectively. In addition, the recovery of Mg in the reduction process reached 99.35%. An analysis of the experimental results also indicated that the addition of CaO could cause the Fe-Si alloy to transform into the Fe-Ni alloy in the nickel-rich residue, which increased the content of Fe-Ni in the magnetic separation material from 13.34% to 73.17%. In addition, the concentration in reduced ore of Si from 45.43% increased to 83.68%, which could reduce the evaporation of Si in the form of SiO at high temperatures. If Si volatilized in the form of SiO during the condensation process, SiO would disproportionate to form Si and SiO₂, contaminated condensed magnesium. In summary, the valuable metals in the minerals were comprehensively utilized with the addition of CaO.

Keywords: Garnierite; Vacuum carbothermal reduction; Additive; Magnetic separation

1. Introduction

Nickel has been a very important metal in the modern world. Nickel-based alloys are widely used in today's technologies and other aspects of life from mobile phones to medical equipment, energy generation and transportation [1-2]. Hence, nickel sulfide ore resources are becoming rapidly depleted and the development and utilization of low-grade nickel laterite ore is gaining attention [3-4].

Smelting methods for nickel laterite ore are divided into three categories: pyrometallurgical, hydrometallurgical, and the pyrometallurgy-hydrometallurgy united metallurgical technology [5-14]. Besides, the study on the application of magnetic

separation technology in metallurgy became more common in recent years [15].

However, these methods are focused only on the recovery of Fe and Ni in minerals. Other valuable metals such as Si and Mg become slag and end up in landfills. This practice is a waste of resources and causes environmental pollution [16-21]. Yunnan Yuanjiang nickel laterite ore is mineral garnierite that is typically composed of 0.83% Ni, 0.08% Co, 11% Fe, 28% MgO, and 37% SiO₂ on average. According to a statement issued by Shanghai Nonferrous Metals Trading Network on April 10th, the value of Ni was 16,062.34 USD/t and the value of Mg was 2,512.72 USD/t, for 100 tons of the raw materials the value of Ni was 13,331.74 USD, and the value of Mg was

*Corresponding author: qutao_82@126.com



40,343.51 USD, where the value of Mg was much greater than the value of Ni. A kinetic study of lizardite, which exists in silicates, indicated that lizardite begins to decompose at 923K and completely decomposes at temperatures greater than 1,073K. However, magnesium silicate is formed after decomposition, and magnesium silicate is extremely difficult to destroy. Therefore, the extraction of magnesium from garnierite has been neglected. Hence, we must explore new technological methods to extract Ni, Fe, and Mg, at the same time, thereby reducing the discharge of metallurgical waste and preventing environmental pollution [22-25].

A previous study on calcium additives in garnierite was conducted, but the valuable metals in the minerals could not be comprehensively utilized [26-31]. The purpose of this work is to explore a new process and provide a highly efficient and energy saving method, named the vacuum carbothermal reduction-magnetic separation method, to comprehensively utilize the garnierite. Additionally, the effect of CaO on the recovery of Fe and Ni in garnierite during vacuum carbothermal reduction would also be explored. The experimental flow chart is shown in Fig. 1.

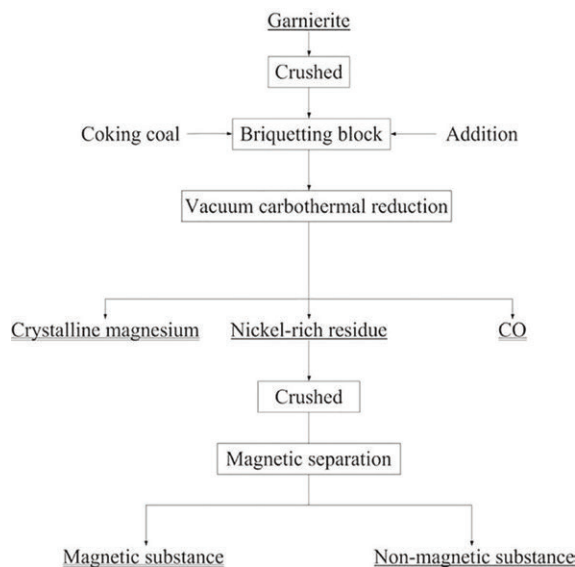


Figure 1. Flow sheet of the experimental procedure

1. Experiment

1.1 Raw materials and equipment

The composition of raw materials, additives, and reducing agents are listed in Tables 1, 2, and 3, respectively. Fig. 2 shows the XRD pattern of the raw materials, with the main components being lizardite and goethite. Fig. 3 represents a schematic diagram of the experimental vacuum furnace. Besides, other

equipment used during the experiment was Planetary ball mill and briquetting machine.

Table 1. The chemical composition of garnierite (wt%)

Elements	Ni	MgO	Fe	SiO ₂	Al ₂ O ₃	Others
Content/%	1.00	28.70	10.52	38.45	2.44	18.89

Table 2. The chemical composition of CaO (wt%)

Component	CaO	Sulfate	Fe	Chloride	Alkali metal	Others
Content/%	≥98.0	≤0.1	≤0.015	≤0.003	≤0.5	≤1.36

Table 3. The chemical composition of coal (wt %)

Elements	Moisture	Ash	Volatile	C	S
Content/%	1.21	30.65	21	47.14	0.42

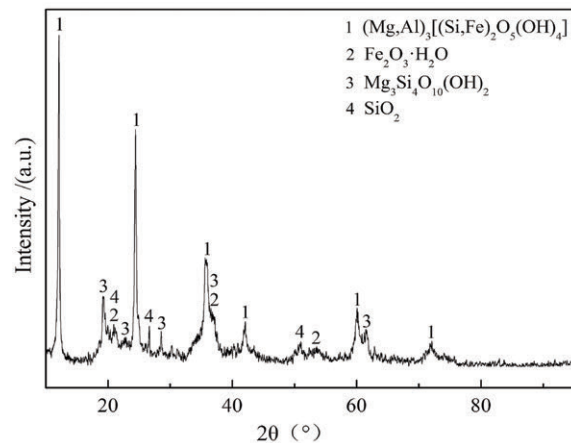


Figure 2. XRD patterns of garnierite

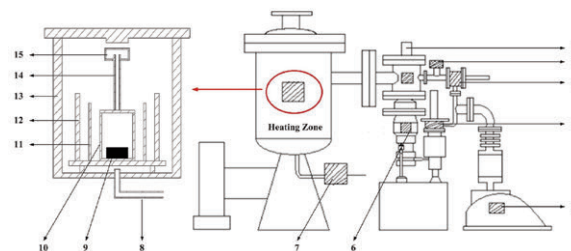


Figure 3. Schematic model of the vacuum distillation furnace 1. High vacuum valve; 2. Release valve; 3. Bypass valve; 4. Main valve; 5. Rotary vane pump; 6. Diffusion pump; 7. Inflation valve; 8. Vacuum pipe; 9. Raw materials; 10. Graphite crucible; 11. Graphite heater; 12. Heat shield; 13. Water cooled walls; 14. Graphite condensing pipe; 15. Condensation

1.2 Experimentation

Coking coal and garnierite were crushed and screened, 100% of the raw materials were less than or

equal to 109 μm, according to the molar ratio of 1:1.2 mixed materials. The following masses of CaO were studied: 0%, 10%, 15%, 20%, 22.64% (the mole ratio of CaO/Si was 1:1), 25%, and 30% for their effect on the experimental results. First, the mixed powder material was pressed into a block and placed in a graphite crucible. Heating was carried out by placing the graphite crucible in a vacuum furnace. The system temperature was raised from room temperature to the desired temperature (1623 K, 1673 K and 1723 K). The cooling water and vacuum pump were shut off after cooling to room temperature.

After cooling, the residue in the crucible was taken out, then the vibrating grinding machine to crush the material to approximately 100 mesh was used. The following step was to put this 100 mesh material into the planetary ball mill for ball milling, according to the required mass, matched into the different size of ball grinding beads, and the ball grinding continued for 4 hours, until the materials thoroughly mixed uniformly. After the ball milling finished, the material was taken out, sampled and sent for detection, and for the remaining part magnetic separation was conducted.

A certain mass of the residue was poured into a container filled with water, which was mixed evenly. Then the small beaker within N45 trademark of neodymium iron was placed into the container so the magnetic material could be absorbed on the outer wall of the beaker. The adsorbed magnetic material was transferred into another basin that contained clear water. The above operation was repeated three times, magnetic and non-magnetic material was separated effectively after three magnetic separations.

The recovery β_1 of the reduction process is expressed as:

$$\beta_1 = M_a / M_0 \tag{1}$$

where M_a and M_0 refer to the mass of metal in the nickel-rich residue and in the ore, respectively.

The recovery β_2 of the reduction magnetic separation process expressed as:

$$\beta_2 = M_b / M_a \tag{2}$$

where M_a and M_b refer to the mass of metal in the magnetic substance and the mass in the nickel-rich residue, respectively.

The recovery β of the total process is expressed as;

$$\beta = \beta_1 \cdot \beta_2 \tag{3}$$

1.3 Analysis methods

The nickel-rich residue was identified by the X-ray diffraction (XRD) with Japan Science D/max-R diffractometer (Cu K α radiation; 40mA; 50kV). The

diffraction angle (2θ) was scanned from 10° to 90° with 4° increments. The morphology and elemental composition of the particular regions were determined by Scanning Electron Microscopy (SEM, HITACHI TM-3030 Plus) equipped with an Energy Dispersive X-ray Spectroscopy (EDS, INCA Oxford). The chemical analysis of nickel-rich residue was performed by inductively coupled plasma atomic emission spectroscopy (ICP-OES) with an Optima 8000 (American, PerkinElmer).

2. Results and discussion

2.1 Reduction process

The direct recovery of Fe and Ni is shown in Fig. 4 and Fig.5, respectively. As can be seen from the figures, the direct recovery of Fe and Ni first increased and then decreased, with maximal direct

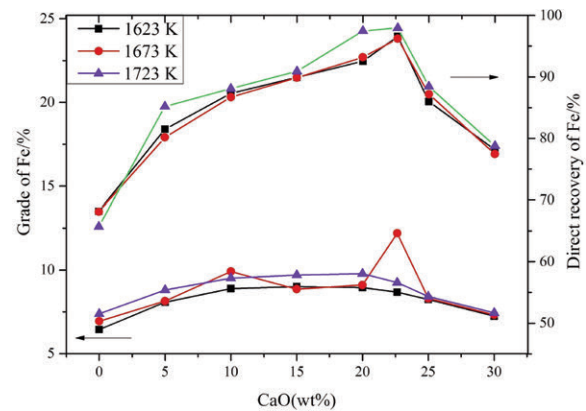


Figure 4. The effect of additives and temperature on Fe enrichment (%), the upper three lines in the figure represents the direct recovery of Fe, and the lower three lines in the figure represents the grade of Fe

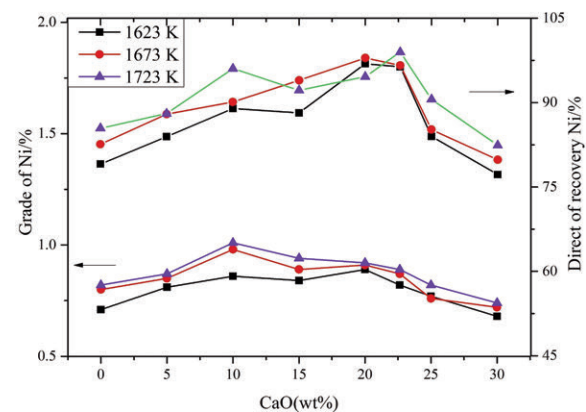


Figure 5. The effect of additives and temperature on Ni enrichment (%), the upper three lines in the figure represents the direct recovery of Ni, and the lower three lines in the figure represents the grade of Ni



recovery achieved at 20% CaO. When the addition of CaO was 22.64%, the direct recovery of Fe and Ni dropped slightly; however, when the addition of CaO was 25% and 30%, the direct recovery of Fe and Ni dropped sharply. The reasons of the results was that when the amount of CaO increased from 0% to 22.64%, all the the added CaO combined with the silicon to form Ca_2SiO_4 , which caused the release of Fe and Ni in the from of silicate and reacted with carbon; nonetheless, with the addition of CaO it continued to increase, the silicon in the raw materials completely reacted with CaO, the excessive CaO coated the raw materials, hindered the progress of the reduction reaction, which caused the decrease of the direct recovery of Fe and Ni. With an increase in temperature, the grades of Fe and Ni tended to increase, but the direct recovery of Fe and Ni showed the cross change. When the addition amount of CaO was 22.64%, maximum direct recovery of Fe and Ni was achieved at 1723 K.

According to the available literature [32], the valuable metals in the raw materials are concentrated in the silicate, and the silicate is difficult to destroy. However, higher temperature is conducive to destroying the structure of the ore and promoting the reduction reaction, which causes the grade of Fe and Ni ascension with the increase of temperature. Although the curve of the direct recovery of Fe and Ni is shown cross change, most of them conform to the law of increasing temperature and increasing the direct recovery. Figure 4 shows that when the amount of CaO increased from 20% to 22.64%, the grade of Fe increased from 8.75% to 12.2%, which is the increase of 3.45%. The reasons for this results was that when the addition of CaO was 22.64%, the silicon in the ore basically combined with CaO, which caused the Fe in the ore to reduce sufficiently. However, when the addition of CaO was excessive or too little, the reduction of Fe was incomplete, thus the Fe grade was reduced. In addition, the phase of the reduced Fe was converted from Fe-Si to Fe-Ni or Fe, which caused the error of chemical analysis to reduce. Besides, the decrease in the grade of the Fe and Ni occurred due to the contents of Fe and Ni in the raw material being constant, with an increase in the amount of CaO, the grades of the Fe and Ni decreased [33].

2.2 Additive effects and thermodynamic analysis

In order to determine the optimal temperature and the amount of CaO, an analysis of the nickel-rich residue phase using XRD was performed as shown in Fig. 6 and Fig. 7.

When CaO was added in the range of 0% to 20%, the main diffraction peak was Fe-Si phase. When the molar ratio of Si/Ca was 1:1, with the addition of CaO

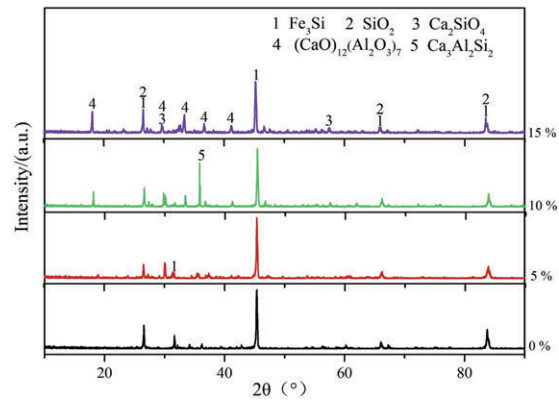
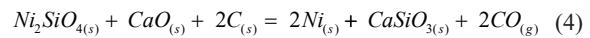
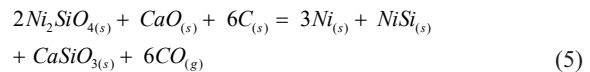


Figure 6. XRD patterns with the addition of 0%-15% CaO at 1723 K

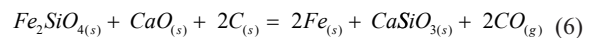
being 22.64%, the Fe-Si phase disappeared, the Fe-Ni and Fe phases appeared, and a large amount of Ca_2SiO_4 formed. For this phenomenon, a thermodynamic analysis was conducted that may have occurred during the reduction process. The four possible reactions for Ni_2SiO_4 and Fe_2SiO_4 are shown in equations (4) to (7) with the relationship of gibbs free energy and temperature. According to the calculation, the initial temperature of samples (4), (5), (6) and (7) were 379.6 K, 730 K, 533.3 K, and 828.5 K respectively, and initial temperature was low, which can explain the formation of Ca_2SiO_4 .



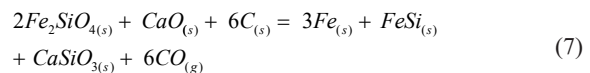
$$\Delta G^\theta = 193.62 - 0.51T \text{ kJ/mol}$$



$$\Delta G^\theta = 1065.74 - 1.46T \text{ kJ/mol}$$



$$\Delta G^\theta = 250.67 - 0.47T \text{ kJ/mol}$$



$$\Delta G^\theta = 1201.29 - 1.45T \text{ kJ/mol} \Delta G^\theta$$

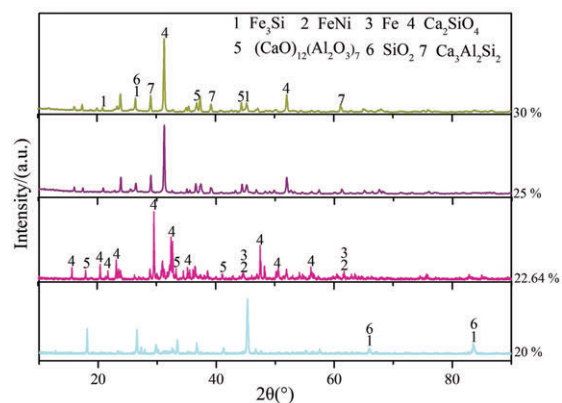
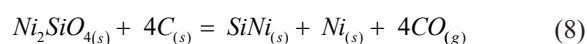
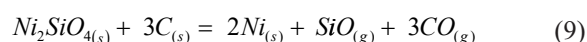


Figure 7. XRD patterns with the addition of 20%-30% CaO at 1723 K

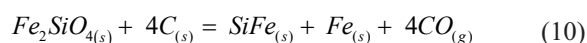
When the addition of CaO was 25% and 30%, the diffraction peak was mainly calcium-containing compound. The reasons of the results was that when CaO was added in amounts ranging from 0% to 20%, the content of Si in the raw material was still larger than the content of Ca. When CaO completely made slag with Si, the materials direct reacted with carbon to form Fe-Si and Ni-Si, so its diffraction peak occurred in the Fe-Si phase, as shown by the equations (8) and (10). Besides, some of the Si evaporated in the form of SiO, as shown by the equations (9) and (11). Therefore, an increase in the amount of CaO could reduce the formation of Ni-Si and Fe-Si, increase the content of Ni%+Fe% in magnetic materials, and prevent the volatilization of silicon.



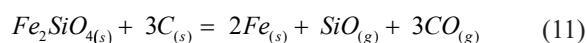
$$\Delta G^\theta = 864.06 - 0.98T \text{ kJ/mol}$$



$$\Delta G^\theta = 955.12 - 0.99T \text{ kJ/mol}$$



$$\Delta G^\theta = 943.06 - 0.93T \text{ kJ/mol}$$



$$\Delta G^\theta = 1033.88 - 0.95T \text{ kJ/mol}$$

When the addition of CaO was 25% and 30%, the excessive CaO coated the raw materials and hindered the progress of the reduction reaction, which lead to the formation of a large amount of silicon-calcium compounds. Therefore, too much or too little of CaO was not conducive to the reduction of Fe and Ni. The results of this analysis are consistent with the results of Section 2.1. In addition, CaO also had significant effect on the recovery of Si and Mg in the reduction process.

In addition, as can be seen from Table 4, with the addition of CaO, the concentration in residue of silicon rose from 45.43% to 83.68%, and most of the Si remained in the nickel-rich residue. This greatly reduced the volatility of Si, and the remove rate of Mg increased from 67.26% to 99.35%. This demonstrated

Table 4. The concentration in reduced ore of Si and the removal rate of Mg at 1723 K with different amounts of CaO (wt%)

Added amount of CaO%	0	5	10	15	20	22.64	25	30
The concentration in residue of Si%	45.43	74.85	77.77	81.81	83.45	83.68	81.17	80.03
The removal rate of Mg%	67.26	97.61	99.96	99.49	99.81	99.35	98.04	98.88

that during the reduction process, CaO preferentially reacted with the silicate to inhibit the formation of olivine and enhanced the reduction of Mg [27,34].

Based on Section 2.1 and analysis of Section 2.2, and considering the comprehensive recovery of each valuable metal, the addition of 22.64% CaO at 1723 K was thought to be the optimal condition.

2.3 SEM/EDS analysis

Fig.8 and Fig.9 show the SEM/EDS images without and with 22.64% CaO at 1723 K, respectively. Fig.8(c) and Fig.9(f) represent the element surface profiles of Fe, Ni, and Si, where the red, green, and blue represent the Fe, Ni, and Si respectively.

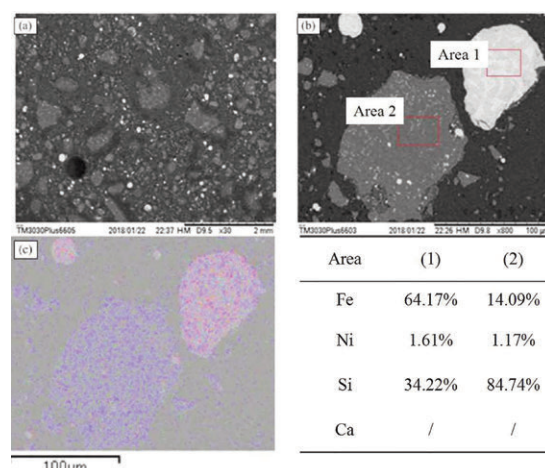


Figure 8. SEM micrograph at 1723 K without CaO, which picture (a) magnified 30 times, (b) and (c) magnified 800 times; and the red, green and blue in picture (c) represent the Fe, Ni and Si respectively

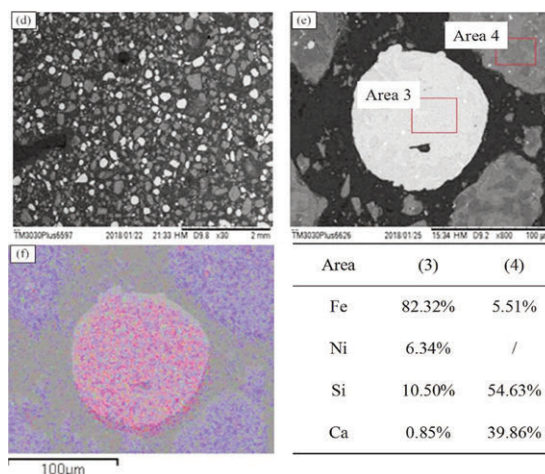


Figure 9. SEM micrograph at 1723 K with 22.64% CaO, which picture (d) magnified 30 times, (e) and (f) magnified 800 times; and the red, green and blue in picture (f) represent the Fe, Ni and Si respectively



As can be seen from Fig.8(b) and the element content, it can be concluded that the white area indicates Fe accumulation, and the grey area indicates Si aggregation. Ni distributed uniformly with no aggregation, and Fe and Si mixed with each other in aggregation area. Fig.9 shows that the white areas indicate Fe and Ni aggregation, and the grey areas represent Si-Ca aggregation. By comparing Fig.8 and Fig.9, it can be seen that in the presence of CaO, Ni would collect in the Fe accumulation area and effectively reduce the Si content. Fig. 8(a) and Fig.9(d) show the size and the amount of Fe aggregate particles in the absence or presence of CaO. It can be seen that at 22.64% CaO, Fe aggregates became significantly larger whatever their size or amount is.

After magnetic separation, as can be seen from Fig.10, the Fe-Ni alloy only contained 6.83% Si and the Si-enriched area only contained 2.41% Fe, indicating that the addition of CaO effectively

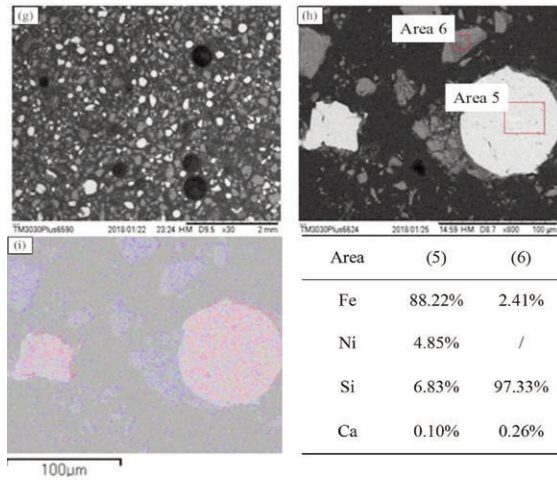


Figure 10. SEM micrograph at 1723 K with 22.64% CaO after magnetic separation, which picture (g) magnified 30 times, (h) and (i) magnified 800 times; and the red, green and blue in picture (i) represent the Fe, Ni and Si respectively

promoted the separation of Fe-Ni, Si, which was favourable for magnetic separation. The conclusions of these analyses demonstrated that the addition of 22.64% CaO at 1723 K was the optimal condition.

2.4 The magnetic separation process

The magnetic separation process data are shown in Table 5. When no CaO is added, there is no non-magnetic material after magnetic separation, and the amount of CaO increased from 0% to 30%, the amount of Fe-Ni increased from 13.34% to 73.17%, and the content of Si decreased from 11.63% to 4.93%. With an increase in CaO, more Si formed Ca₂SiO₄ and the content of Si was reduced in the magnetic material, thereby reducing the proportion of magnetic material in the nickel-rich residue.

Table 6. Enrichment ratio of Ni and Fe with different dosages of CaO at 1723 K during the vacuum carbothermal reduction-magnetic separation process

Added amount of CaO (wt%)	0	5	10	15	20	22.64	25	30
Enrichment ratio of Fe	1.15	3.79	3.83	5.77	5.75	6.32	5.97	6.04
Enrichment ratio of Ni	1.22	4.20	4.32	6.60	6.48	6.72	6.63	6.21

Table 7. The recovery of Fe and Ni in the magnetic separation process at 1723 K

Added amount of CaO(wt %)	0	5	10	15	20	22.64	25	30
Recovery of Fe (%)	100	98.29	97.67	99.03	94.94	86.08	90.21	92.15
Recovery of Ni (%)	100	96.46	98.02	97.80	97.80	98.78	97.26	99.03

Table 5. The content and mass of each metal in the magnetic material, non-magnetic material in the magnetic separation process at 1723 K

CaO /wt%	Mass of residue/g	Mass of magnetic material/g	The content of elements in the magnetic material/%			Mass of nonmagn-etic material/g	The content of elements in the non-magnetic material/%		
			Fe	Ni	Si		Fe	Ni	Si
0	31.64	31.64	12.12	1.22	11.63	0	0	11.63	
5	32.59	6.78	39.90	4.20	6.84	25.81	0.22	15.61	
10	30.08	6.92	40.24	4.32	6.07	23.16	0.30	14.94	
15	32.81	4.86	60.71	6.60	5.39	27.95	0.58	14.62	
20	34.63	5.05	60.50	6.48	5.17	29.58	0.53	12.82	
22.64	33.64	4.21	66.45	6.72	4.93	29.43	1.31	12.27	
25	34.40	4.15	62.78	6.63	4.89	30.25	0.97	11.25	
30	33.70	3.97	63.56	6.21	4.99	29.73	0.62	14.03	



Table 8. The recovery of Fe and Ni during the vacuum carbothermal reduction-magnetic separation process at 1723 K

Added amount of CaO(wt %)	0	5	10	15	20	22.64	25	30
Recovery of Fe (%)	65.72	83.73	87.71	90.04	92.54	84.33	79.78	71.03
Recovery of Ni (%)	85.45	84.93	90.36	92.51	96.80	97.00	88.09	81.63

From the data in Tables 5, 6, 7, and 8, it can be seen that with CaO increase, the enrichment ratio of Fe and Ni gradually increased. When the addition of CaO was 22.64%, the enrichment ratio of Fe and Ni was the largest, reaching 6.32 and 6.72 times, respectively. The magnetic separation direct recovery of Fe and Ni were 86.08% and 98.78%, respectively, and the magnetic direct recovery of Ni reached the maximum. The recovery of Ni during the vacuum carbothermal reduction-magnetic separation process reached a maximum of 97.00%, and the recovery of Fe was 84.33%. The analysis shown that the addition of CaO can promote the separation of Si and Fe-Ni during the carbothermal reduction process, thereby reducing the content of Si in the magnetic material and increasing the recovery of the Fe and Ni.

3. Conclusions

1) The experimental results demonstrated that when CaO was added in ranging from 0% to 30%, the nickel-rich slag phase changed from Fe-Si to Fe-Ni, making the content of Fe-Ni in the magnetic separation material increase from 13.34% to 73.17%, effectively increasing Fe-Ni content in the magnetic materials. In addition, the concentration in reduced ore of Si from 45.43% increased to 83.68%, which could reduce the evaporation of Si in the form of SiO at high temperatures. If Si volatilized in the form of SiO during the condensation process, SiO would disproportionate to form Si and SiO₂ contaminated condensed magnesium.

2) The addition of CaO increased the removal rate of Mg from 67.26% to 99.35%, which indicated that during the reduction process, CaO preferentially reacts with SiO₂ to form Ca₂SiO₄ and inhibited the formation of olivine and enhanced the reduction of Mg.

3) The experiments indicated that the optimal conditions for the recovery of Fe and Ni occurred when the temperature was 1723 K, the mass ratio of ore/C was 100:65.5, and the CaO content was 22.64% (the molar ratio of CaO/Si is 1:1). The recovery of Fe and Ni in the whole process reached 84.33% and 97.00%, and the enrichment ratio of Fe and Ni reached a maximum of 6.32 and 6.72 respectively.

Acknowledgments

This work was supported financially by: (a) National Nature Science Foundation of China (No. 51604133); (b) Academician Free Exploration Fund of Yunnan Province, China (No. 2018HA006).

References

- [1] Y. Liu, Y. Cao, L. Huang, M. Gao, H. Pan, J. Alloy. Compd., 509 (3) (2011) 675-686.
- [2] P.K. H, N.C. W, T. Metal. Mater., Eng. 21 (2008) 1-9.
- [3] D. Uliana, M. Manuela M. LéTassinari, H. Kah, M.A. Angora, Acta Miner. Sin., 33 (S1) (2013) 17.
- [4] B.K. Loveday, Miner. Eng., 21 (7) (2008) 533-538.
- [5] X. Guo, D. Li, K.-H. Park, Q. Tian, Z. Wu, Hydrometallurgy, 99 (2009) 144-150.
- [6] J. Forster, C.A. Pickles, R. Elliott, Miner. Eng., 88 (2016) 18-27.
- [7] S. Kursunoglu, M. Kaya, Int. J. Min. Met., Mater., 22 (11) (2015) 1131-1140.
- [8] S. Agatzini-Leonardou, I.G. Zafiratos, D. Spathis, Hydrometallurgy, 74 (2004) 259-265.
- [9] Y. Zhao, J.-m. Gao, Y. Yue, B. Peng, Z.-q. Que, M. Guo, M. Zhang, Int. J. Min. Met. Mater., 20 (2013) 612-619.
- [10] G.-l. Zheng, D.-q. Zhu, J. Pan, Q.-h. Li, Y.-m. An, J.-h. Zhu, Z.-h. Liu, J. Cent. South U., 21 (2014) 1771-1777.
- [11] R.G. McDonald, B.I. Whittington, Hydrometallurgy, 91 (2008) 35-55.
- [12] I. Quaiocoe, A. Nosrati, W. Skinner, J. Addai-Mensah, Miner. Eng., 65 (2014) 1-8.
- [13] J. MacCarthy, A. Nosrati, W. Skinner, J. Addai-Mensah, Miner. Eng., 77 (2015) 52-63.
- [14] Y. Chang, K. Zhao, B. Pesic, J. Min. Metall. Sect. B-Metall., 52 (2) B (2016) 127 - 134.
- [15] D. Xu, Y. Liu, J. Li, Y.C. Zhai, J. Northeast. Univ., 31 (4) (2010) 559-563.
- [16] E. Peek, A. Barnes, A. Tuzun, Miner. Eng., 24 (2011) 625-637.
- [17] O. J, I. T, Int. J. Miner. Process., 19 (1) (1987) 25-42.
- [18] M. Pelino, A. Karamanov, P. Piscicella, S. Crisucci, D. Zonetti, Waste Manage., 22 (8) (2002) 945-949.
- [19] X.-h. Tang, R.-z. Liu, L. Yao, Z.-j. Ji, Y.-t. Zhang, S.-q. Li, Int. J. Min. Met. Mater., 21 (10) (2014) 955-961.
- [20] X. Ma, Z. Cui, B. Zhao, JOM-US, 68 (12) (2016) 3006-3014.
- [21] Z.-M. Li, T. Zhu, J.-Z. Wu, Chin. J. Nonferrous Met., 2 (1) (2009) 29-32.
- [22] S. Zhou, Y. Wei, B. Li, B. Ma, C. Wang, H. Wang, J. Alloy. Compd., 7 13 (2017) 180-186.
- [23] M.G. King, J. Alloy. Compd., 57 (2005) 35-39.
- [24] K. Quast, J.N. Connor, W. Skinner, D.J. Robinson, J. Addai-Mensah, Miner. Eng., 79 (2015) 261-268.
- [25] J.-M. Gao, M. Zhang, M. Guo, Hydrometallurgy, 158 (2015) 27-34.
- [26] Q. Luo, T. Qu, D. Liu, Y. Tian, B. Yang, Y. Dai, Vac. Sci. Technol., 32 (5) (2012) 430-436.
- [27] Q. Luo, T. Qu, D. Liu, Y. Tian, B. Yang, Y. Dai, Vac.



- Sci. Techno., 32 (11) (2012) 1026-1032.
- [28] J. Luo, G. Li, Z. Peng, M. Rao, Y. Zhang, T. Jiang, JOM-US, 68 (12) (2016) 3015-3021.
- [29] S. Zhou, Y. Wei, B. Li, H. Wang, B. Ma, C. Wang, Metall. Mater. Trans. B., 47 (1) (2015) 145-153.
- [30] Y.-q. Chen, H.-l. Zhao, C.-y. Wang, Int. J. Min. Met. Mater., 24 (5) (2017) 512-522.
- [31] X.-M. Lv, X.-W. Lv, L.-W. Wang, J. Qiu, M. Liu, J. Min. Metall. B., 53 (2) (2017) 147 - 154.
- [32] B. Ma, C. Wang, Y. Wei, H. Wang, W. Yang, Rare Metals., 41 (04) (2017) 429-436.
- [33] B. Li, H. Wang, Y.-G. Wei, Miner. Eng., 24 (2011) 1556-1562.
- [34] Q. Luo, T. Qu, D. Liu, B. Xu, B. Yang, Y. Dai, J. Cent. South. Univ., 43 (11) (2012) 4190-4198.

UTICAJ CaO NA DOBIJANJE Fe I Ni KARBOTERMIČKOM REDUKCIJOM GARNIJERITA U VAKUUMU

Q. Wang ^{b,c,d}, T. Qu ^{a,b,c,d*}, X.-P. Gu ^{a,b,c,d}, L. Shi ^{b,c,d}, B. Yang ^{a,b,c,d}, Y.-N. Dai ^{b,c,d}

^a Glavna državna laboratorija za potpuno iskorišćenje resursa složenih obojenih metala, Univerzitet nauke i tehnologije u Kunmingu, Kunming, Kina

^b Nacionalna inženjerska laboratorija za vakuumsku metalurgiju, Univerzitet nauke i tehnologije u Kunmingu, Kunming, Kina

^c Glavna laboratorija za vakuumsku metalurgiju obojenih metala iz provincije Junan, Univerzitet nauke i tehnologije u Kunmingu, Kunming, Kina

^{d*} Fakultet metalurškog i energetskog inženjerstva, Univerzitet nauke i tehnologije u Kunmingu, Kunming, Kina

Apstrakt

U ovom radu je ispitivan uticaj dodavanja CaO na prinose Fe i Ni tokom postupka karbotermičke redukcije u vakuumu. Pored toga je ispitana i magnetna separacija. Eksperimenti su sprovedeni pod različitim pritiscima od 10 do 50 Pa sa različitim razmerama CaO i na različitim temperaturama. Rezultati pokazuju da je pri masenom udelu rude i C od 100:65,5 na temperaturi od 723K kada je udeo CaO bio 22,64% (molarni odnos CaO/Si je bio 1:1), količina dobijenog Fe i Ni dostigla 84,33% i 97,00% prilikom postupka karbotermičke redukcije u vakuumu i magnetne separacije, a da je stepen zasićenja bio maksimalan i da je iznosio 6,32 i 6,72. Dobijena količina Mg prilikom postupka redukcije je dostigla 99,35%. Analiza eksperimentalnih rezultata je takođe pokazala da dodavanje CaO može da transformiše Fe-Si leguru u Fe-Ni leguru u ostatku bogatom Ni, što povećava sadržaj Fe-Ni prilikom magnetne separacije materijala sa 13,34% na 73,17%. Pored toga, koncentracija Si u redukovanoj rudi se povećala sa 45,43% na 83,68%, što može da smanji isparavanje Si u obliku SiO na visokim temperaturama. Kada bi Si ispario u obliku SiO tokom procesa kondenzacije, SiO bi nesrazmerno formirao Si i SiO₂ i nečisti kondenzovani Mg. Sve u svemu, vredni metali u mineralima su sveobuhvatno iskorišćeni dodavanjem CaO.

Ključne reči: Garnijerit; Karbotermička redukcija u vakuumu; Primesa; Magnetna separacija.

